Investigation of Stress in AlN Thin Films for Piezoelectric MEMS

R. E. Sah*, L. Kirste*, M. Baeumler*, P. Hiesinger*, V. Cimalla*, V. Lebedev*, F. Knöbber*, O. Bludau*, C. C. Röhlig*, and H. Baumann**

*Fraunhofer Institute for Applied Solid State Physics, Tullastr, 79108 Freiburg, Germany, sah@iaf.fhg.de
**J. Goethe Universität, Institut für Kernphysik, Max-von-Lauer-Str. 1, 60438 Frankfurt, Germany

ABSTRACT

In this contribution, the mechanical stress and the Young's modulus of highly textured aluminum nitride (AlN) films are investigated on (i) thin films, (ii) on thin membranes and (iii) on resonant microstructures. Aging and thermal cycling experiments reveal that stoichiometric AlN thin films are highly stable, while nitrogen deficient AlN films get oxidized in the atmosphere which results in change in the as-grown stress with aging. The fabricated suspended AlN microstructures show an outstanding high stability even for high bending forces. All the employed techniques yield the value for the Young's modulus in the range of 310-350 GPa. The residual stress of the films and membranes is 300-450 MPa, while lower values were obtained for suspended microstructures. The good stability of stress with aging, the stability of microstructures, and the piezoelectric properties indicate that the devices will be highly reliable without any deterioration in their performance, which could be related to the stress.

Keywords: stress analysis, piezoelectric MEMS, AlN membranes, microresonators

1 INTRODUCTION

Wurtzite type AlN thin films have become of great interest in micro- and nanoelectromechanical systems (MEMS and NEMS), that have found unique applications in sensing, telecommunications, signal processing, data storage and more [1-6]. As-grown films always have a residual stress. The magnitude and sign (tensile or compressive) of the residual stress vary depending on the deposition conditions [7,8]. For most applications, the residual stress has to be minimized because it alters the bending in MEMS. It can also influence the film properties, hence, the characteristics of devices. On the other hand, some devices, such as resonant strain sensors, require residual tensile stress for proper operation [9,10]. Thus, in order to achieve desired properties of MEMS and NEMS, and for the reliability of these devices, an investigation of the residual stress and its stability is important. Recently, we have demonstrated the stress stability for thin stoichiometric AlN films [11]. In this contribution, we extend this study by including the analysis of suspended microstructures, such as membranes, cantilevers and microbridges and demonstrate the stress stability and hence reliability of the piezoelectric devices.

2 EXPERIMENTAL

The AlN films were grown on 3" Si(001) substrate in a commercial radio frequency (rf=13.56 MHz) magnetron sputtering system. Details can be found in Ref. [11]. Post growth thermal cycling was performed between room temperature and 400°C in N_2 atmosphere. The thickness of the film was determined using Variable-Angle Spectroscopic Ellipsometer (Woolam Co.). Measurements were performed in a wide spectral range, from 190 nm (6.52 eV) to 1700 nm (0.73 eV), at three different incident angles, 65°, 70° and 75°. This thickness was confirmed by X-Ray Reflectivity (XRR) measurements.

The stoichiometry of the film was determined by Energy Dispersive X-ray (EDX) and Rutherford Backscattering Spectroscopy (RBS) techniques. The structural analysis including the surface roughness and density were performed by X-Ray Diffraction (XRD) and XRR measurement techniques. The piezoelectric coefficient, d_{33}, was determined by laser vibrometry with a precision of about 1 pm.

Stress and Young's modulus of the AlN films were determined by three different methods. First, by scanning laser reflection (SLR) the curvature of the Si substrate was measured. To convert the curvature to stress, the modified Stoney equation [12],

$$\sigma = \frac{E_s\, t^2}{6\,(1-\upsilon_s)\, d}\left(\frac{1}{R}-\frac{1}{R_0}\right), \qquad (1)$$

has been used, where E_s, ν_s, and t are Young´s modulus, Poisson´s ratio and the thickness of the substrate, respectively, and R, R_0 are measured radii of curvature of the wafer before and after deposition of the films of thickness d.

Second, the residual stress in the films has been deduced from bulging experiments on freestanding AlN membranes using the relation [13,14]:

$$p = p_0 + \frac{c_1 \cdot d}{r^2}\cdot\sigma_0\cdot z + \frac{c_2\cdot f(\upsilon)\cdot d}{r^4}\cdot\frac{E}{1-\upsilon}\cdot z^3, \qquad (2)$$

where p is the uniform pressure applied to the membrane, r is the membrane radius, d is the membrane thickness, z is the maximum deflection measured at the center of the hemispherical membrane, and $\nu = 0.24$ is the Poisson´s ratio. The geometrical coefficients c_1, c_2, and $f(\nu)$ for circular membranes are 4, 2.67, and 1, respectively.

Third, mechanical microresonators in the shape of cantilevers and doubly clamped bridges have been fabricated using AlN films and an Al metallization with a thickness of 200 nm and 50 nm, respectively [2,15]. Typically these resonators had a length L of 10-500 µm and a width w of 1 – 12 µm. The resonant frequencies of these microresonators have been determined using magnetomotive (Lorentz-force) or external piezoelectric excitation and a displacement measurement by a laser vibrometry method. The measurements were analyzed analytically using the Euler-Bernoulli theory:

$$f_{0n} = (k_n^2 / 4\pi\sqrt{3})\sqrt{E/\rho}(d/L^2)\sqrt{1+\gamma_n\varepsilon\left(L^2/d^2\right)}, \qquad (3)$$

where ρ=3.255 g cm^{-3} is the density of the film, n is the mode number, k_n and γ_n are mode dependent prefactors [16]. The residual strain ε is relevant only for doubly clamped bridges, while cantilevers are assumed to be relaxed.

3 RESULTS AND DISCUSSION

Using spectroscopic ellipsometry, parameters Ψ and Δ were recorded. The data were fitted to different layered structures, air/AlN/Si(001), air/AlN/SiO_2/Si(001), and surface roughness/AlN/Si(001). The thickness of the SiO_2 at the interface was found to be zero. The surface roughness and a possible surface oxidation of the AlN are described by an effective medium approximation of the AlN layer containing 50 % voids. The dielectric function of AlN was modeled by two parametric oscillator functions [17] at energies of E_0=6.2 eV and E_1=7.8 eV to account for the band edge and the E_1 transitions [18]. With respect to crystalline AlN, the transitions are characterized by enhanced broadening parameters. The calculations revealed that the thickness and the refractive index of the film were 164 nm and 2.02, respectively.

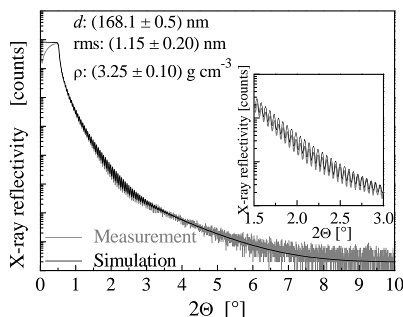

Fig. 1: XRR measurements and simulation of a stoichiometric AlN film grown on Si(001).

Fig. 1 shows the measurement and simulation of XRR scans probed by CuKα radiation. The simulation of the XRR scans yielded a film thickness value of 168 nm, which is in a good agreement with the ellipsometric value given above. Furthermore, the simulation yielded a root mean square surface roughness, rms, of 1.15 nm and a film density, ρ, of 3.25 g/cm³.

Fig. 2 shows a typical XRD pattern ($\Theta/2\Theta$-scan) of AlN/Si(001) structures. The AlN related peaks are indexed on the basis of the hexagonal geometry of the unit cell. In addition to the 004 reflection of the Si(001) substrate, the pattern shows the 00.2, 00.4 and 00.6 reflections of AlN. The fact that only AlN reflections of the type 00.L are detected and furthermore, the reflections other than the AlN 00.L-type are absent, indicates that the AlN grains are preferably oriented along the c-axis perpendicular to the film surface. From the 00.2 peak the c lattice parameter was determined to be about 4.98 Å, which is in a good agreement with 4.982 Å given in the literature [2]. Cross sectional scanning electron microscopy (SEM) and XRD pole figure measurements confirmed the fiber texture of the AlN films [11]. Rocking curves were recorded around the 00.2 Bragg reflection. The relatively small value, 3.55°, for the FWHM for stoichiometric AlN/Si(001) indicates good crystal orientation, i.e., the tilt of grains away from the perpendicular to the surface is low.

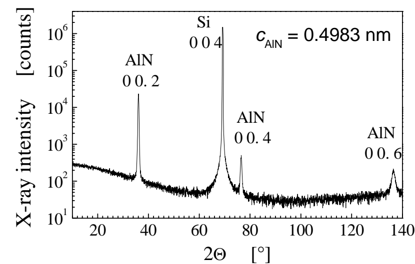

Fig. 2: XRD $\Theta/2\Theta$ pattern of 200 nm thick AlN on a Si(001) substrate.

Fig. 3 illustrates the EDX measurement of the stoichiometric AlN film. Only Al and N signals could be detected in the sample. The extremely week signal of oxygen proves that the film hardly absorbs atmospheric water or oxygen. The composition of this film is calculated to be 50.7 at% N, 48.8 at% Al, and 0.5 at% O. The RBS measurements confirmed these values [11].

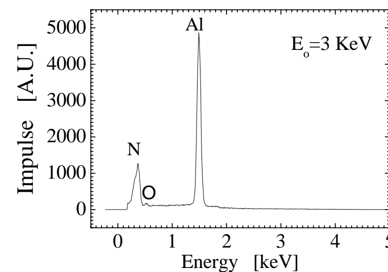

Fig. 3: EDX spectrum of a stoichiometric AlN film.

Fig. 4 depicts the change in stress on aging for a slightly nitrogen-rich (referred as stoichiometric) film grown at the flow ratio of $Ar:N_2$=70:40 sccm and the slightly nitrogen-deficient (referred as non-stoichiometric) film grown at the flow ratio of $Ar:N_2$=70:15 sccm. The thicknesses of the two films were identical. The as-deposited stress in the stoichiometric film does not change when exposed to the atmosphere following deposition. The as-deposited tensile stress in the film grown with lower flow rate of nitrogen was slightly tensile, which changed to compressive within a couple of hours when exposed to the atmosphere following deposition. Although the XRD Θ/2Θ patterns were very similar for both films, the RBS measurements revealed that the non-stoichiometric film contains 3.2 at% oxygen which apparently got incorporated into the film due to oxidation when exposed to the atmosphere [11]. The growth rates of the stoichiometric and non-stoichiometric films were 16 nm/min and 25 nm/min, respectively. It is anticipated that the relatively high growth rate in the absence of sufficient amount of excited nitrogen species is the main reason for non-stoichiometry.

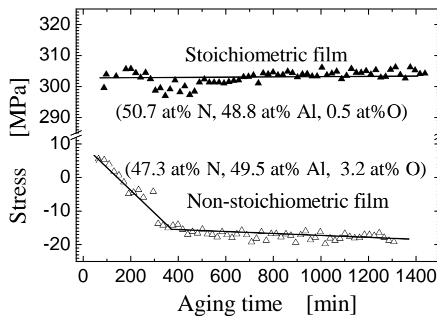

Fig. 4: Aging of stoichiometric and non-stoichiometric AlN/Si(001) at room temperature.

Fig. 5 shows linear decreasing of the stress in the stoichiometric AlN film due to heating from room temperature to 400°C. Upon subsequent cooling from 400°C to room temperature the stress changes follow the same path as of heating, thus, exhibit no hysteresis. The elastic behavior indicates that the device will be reliable in the above temperature range without deterioration of their performances, which could be related to the stress.

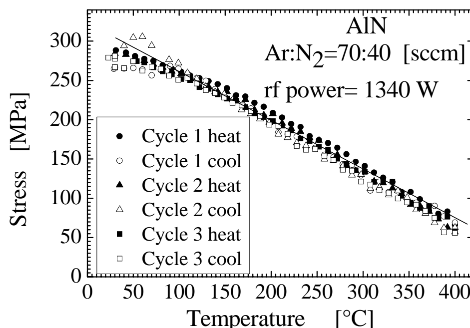

Fig. 5. Temperature cycle dependence of stress in stoichiometric AlN films grown on Si(001) [11].

Mechanical microstructures have been fabricated from the stoichiometric AlN films. Fig. 6 shows the SEM image of an AlN circular membrane of 3 mm in diameter at the bottom of the Si substrate, fabricated by the conventional lithography and plasma-based dry etching.

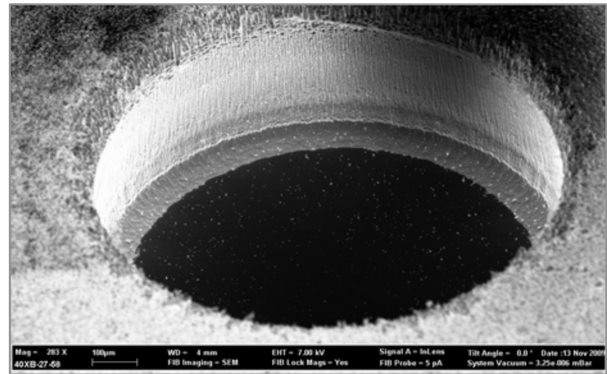

Fig. 6: SEM image of an AlN membrane fabricated by a deep reactive ion etching process.

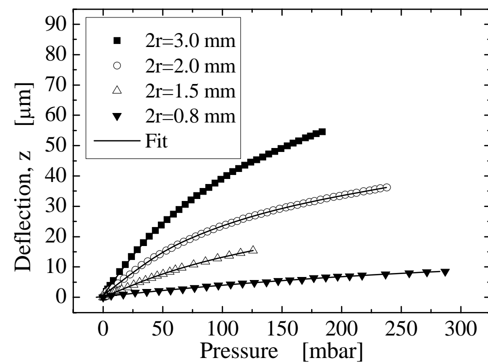

Fig. 7: Load-deflection curves measured by bulging of 200 nm thick AlN membranes of various diameters 2*r*.

The variation of the deflection, *z* of the center with hydrostatic pressure applied on one side of the membrane is shown in Fig. 7. A relatively large deflection already at a low pressure has been observed. By fitting the experimental data to the equation (2), values of the residual stress and Young´s modulus are obtained to be 410 MPa and 336 GPa, respectively. The Young's modulus is in good agreement with those given in the literature [2,19,20], which were obtained for single-crystal AlN.

Finally, resonant oscillating microstructures were analyzed. For the determination of Young's modulus, cantilevers were employed, where the residual stress is assumed to be zero (strain $\varepsilon = 0$ in equation (3)). The results for the first vibration mode as a function of the geometry factor (d/L^2) are shown in Fig. 8. From these data, the Young´s modulus E is calculated to be 310 GPa. Moreover, from the linear fit of the experimental data (Fig. 8) sound wave propagation velocity, $\sqrt{E/\rho}$, is determined to be 9760 m/s, which is in a good agreement with the value

NSTI-Nanotech 2010, www.nsti.org, ISBN 978-1-4398-3402-2 Vol. 2, 2010

given in the literature. Using these values, the resonant behavior of doubly clamped microbridges has been analyzed and the residual stress has been calculated to be 270 MPa.

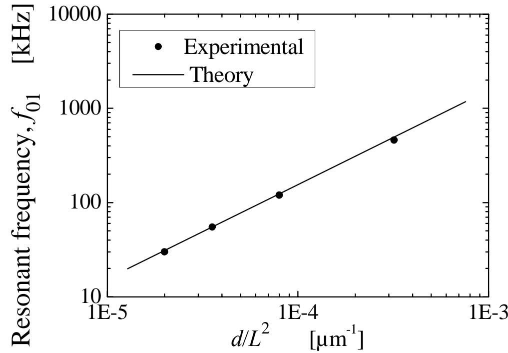

Fig. 8: The first mode resonant frequency as a function of cantilever geometry factor.

Object of measurement	Al/Si(001)	Membrane	Cantilever /Bridges
Measurement technique	SLR	Bulge	Resonant frequency
σ [MPa]	310	410	270
E [GPa]	342	336	310
d_{33} [pm/V]	5.5		

Table 1: Summary of mechanical properties of our AlN obtained by different methods.

Table 1 summarizes the results of measurements of the mechanical properties of AlN carried out on free-standing membranes, films and on microcantilevers. Also included in the Table is the piezoelectric coefficient d_{33}. The high value of d_{33} indicates an excellent piezoelectric property of our AlN film.

4. CONCLUSIONS

The aging and thermal cycles dependences of the mechanical stress in rf sputtered wurtzite-type AlN films revealed that the stoichiometry of the film is an important factor. Thermally induced stress changes in stoichiometric films exhibit no hysteresis with thermal cycles. A stress reduction is observed on free-standing microstructures. The bulge test performed on a stoichiometric AlN membrane shows an extremely sensitive dependence of the deflection on pressure. The Young's modulus of sputtered AlN measured on (i) thin films, (ii) on thin membranes and (iii) on resonant microstructures was determined to be in the range of 310-350 GPa, which is in a good agreement with literature. The good stability of stress with aging, the stability of the microstructures and the piezoelectric properties indicate that the devices will be highly reliable without any deterioration in their performance, which could be related to the stress. Due to these unique properties, the sputtered AlN film is a promising material for reliable sensors.

ACKNOWLEDGEMENTS

Authors are grateful to R. Driad for stimulating discussions, and to O. Ambacher for continued interest, encouragement and support. The work was supported by Fraunhofer grant (ATTRACT), by DFG (projects No. CI148/2 and AM105/9), and by BMBF (project AINTEN).

REFERENCES

[1] A. T. Sowers, J. A. Christman, M. D. Bremser, *et al.*, Appl. Phys. Lett. **71**, 2289, 1997.

[2] V. Cimalla, J. Pezoldt, and O. Ambacher, J. Phys. D, Appl. Phys. **40**, 6386, 2007.

[3] V. Mortet, O. Elmazria, M.Nesladek, *et al.*, Appl. Phys. Lett. **81**, 1720, 2002.

[4] T. Matsutani, M. Kiuchi, K. Shirouzu, *et al*., Solid State Phenom. **107**, 43, 2005.

[5] Y. Taniyasu, M. Kasu, and T. Makimoto, Nature **441**, 325, 2006.

[6] J. Li, Z. Y. Fan, R. Dahal, M. l. Nakarmi, J. Y. Lin, and H. X. Jiang, Appl. Phys. Lett. **89**, 213510, 2006.

[7] G. Este, and W. D. Westwood, J. Vac. Sci. Technol. A **5**, 1892, 1987.

[8] W. J. Meng, J. A. Sell, G. L. Eesley, and T. A. Perry J. Appl. Phys. **74**, 2411, 1993.

[9] K. Ikeda, H. Kuwayama, T. Kobayashi, *et al.*, *Sensors Actuators* A **21/23,** 1007–10, 1990.

[10] T. Yoshida, T. Kudo, S. Kato, *et al.*, *Proc. MEMS '95 (Amsterdam),* 316–21, 1995.

[11] R. E. Sah, L. Kirste, M. Baeumler, *et al.*J. Vac. Sci. Technol. A **28**, 394, 2010.

[12] G. G. Stoney, Proc. R. Soc. London, Ser. A **82**, 172, 1909.

[13] S. Timoshenko and S. Woinowsky-Krieger, "Theory of Plates and Shells," McGraw-Hill, New York, 1959.

[14] E. I. Bromley, J. N. Randall, D. C. Flanders, and R. W. Mountain, J. Vac. Sci. Technol. B **1**, 1364, 1983.

[15] V. Cimalla, C. Foerster, F. Will, *et al.* Appl. Phys. Lett. **88** , 253501, 2006.

[16] K. Brueckner, V. Cimalla, F. Niebelschütz, *et al.* J. Micromech. Microeng. **17**, 2016, 2007.

[17] B. Johs, C. M. Herzinger, J. H. Dinan, A. Cornfeld, and J. D. Benson, Thin Solid Films **313**, 137, 1998.

[18] R. Goldhahn, C. Buchheim, P. Schley, *et al.* in Nitride Semiconductor Devices: Principles and Simulation, ed. J. Piprek, Wiley, Heidelberg, 2007.

[19] K. Tsubouchi and N. Mikoshiba, IEEE Trans. Sonics Ultrason. **SU-32**, 634, 1985.

[20] A. F. Wright, J. Appl. Phys. **82**, 2833, 1997.